UCLA
UCLA Electronic Theses and Dissertations

Title

Increasing the accuracy of CRISPR/Cas9 gene editing for introns 44 and 55 of the DMD gene by using high fidelity Cas9 nucleases

Permalink

https://escholarship.org/uc/item/4nq8b7np

Author

Popack, Dovber

Publication Date

2021

Peer reviewed|Thesis/dissertation

eScholarship.org Powered by the California Digital Library
University of California

UNIVERSITY OF CALIFORNIA

Los Angeles

Increasing the accuracy of CRISPR/Cas9 gene editing for introns 44 and 55 of the *DMD* gene by using high fidelity Cas9 nucleases

A thesis submitted in partial satisfaction

of the requirements for the degree Master of Science

in Physiological Science

by

Dovber Popack

2021

ABSTRACT OF THE THESIS

Increasing the accuracy of CRISPR/Cas9 gene editing for
introns 44 and 55 of the *DMD* gene by using high fidelity Cas9 nucleases

by

Dovber Popack

Master of Science in Physiological Science

University of California, Los Angeles, 2021

Professor Melissa J. Spencer, Chair

Sixty percent of mutations causing Duchenne muscular dystrophy (DMD) occur within introns 44-55 of the *DMD* gene. The Spencer and Pyle Labs have designed a CRISPR/Cas9 platform that deletes introns 44 and 55 of the *DMD* gene to mimic a mild Becker muscular dystrophy (BMD) phenotype. This study compares the efficacy of two different Cas9 nucleases (either eSpCas9 or HypaCas9) in vitro to determine their respective efficiencies in comparison to wild type SpCas9. The data showed that editing efficiency of HypaCas9 was less efficient than either eSpCas9 or wild type SpCas9. Upon sequencing, it was revealed that the eSpCas9 plasmid sent from a company was actually identical to wild type SpCas9. Therefore, though we were not able to assess the efficiency of eSpCas9, the data revealed that hypaCas9 will not be a suitable substitute for wild type Cas9 due to its low efficiency.

The thesis of Dovber Popack is approved.

Amy Catherine Rowat

Rachelle Hope Crosbie-Watson

Melissa J. Spencer, Committee Chair

University of California, Los Angeles

2021

DEDICATION

I would like to dedicate this thesis to God, for giving me the strength and courage to persevere.

TABLE OF CONTENTS

LIST OF FIGURES

ACKNOWLEDEGMENTS

I would like to thank my mentor, Dr. Melissa J. Spencer, for allowing me into the Spencer Lab and supporting my work through these past two years. I was blessed and fortunate to have the opportunity to study in the Spencer Lab. Dr. Spencer was dedicated, kind, and understanding. She was strong, empathetic, and professional, and under her supervision I have grown enormously, not just professionally but personally, as well. So thank you, Dr. Spencer, for everything you have done for me.

Additionally, I would like to express my gratitude to the other members of my committee. Thank you, Dr. Rachelle Hope Crosbie-Watson, for working with me on my project and reviewing my experiments. Dr. Amy Catherine Rowat, thank you for guiding me through my presentations in your classes, and always being available for me.

I would also like to thank Dr. Irina Kramerova for taking the time out of her busy schedule to mentor me as I progressed through this project. Her patience, understanding, and expertise have helped my development as a researcher in a way I could never have dreamed of before. The training I have had under your guidance, Dr. Kramerova, will carry on with me long after graduation. You went above and beyond to help me, and for that I am forever grateful.

Thank you, Michael Emami, for your time and energy, as well as your constant knowledge and advice over these past two years.

I would also like to thank the other members of the Spencer Lab. It was an honor and privilege to work with you all and get to know you. I have learned something from each of you, and I appreciate and will forever cherish my time with you all.

BACKGROUND

Duchenne muscular dystrophy (DMD) is an X-linked recessive disorder, caused by a mutation in the *DMD* gene, which is located on chromosome Xp21 and is the largest gene in the human genome. *DMD* is composed of 79 exons and is about 2.5 million base pairs [1, 2]. The *DMD* gene is associated with several different promotors, each determining the location of expression. Three promotors control the full-length dystrophin transcription; in the brain - B(Dp427b) - in skeletal muscle and cardiac muscle - M(Dp427m) - and in purkinje cells in the cerebellum - P (Dp427p) [2,3]. Other internal promotors of the *DMD* gene lead to expression of truncated forms of dystrophin.

The transcription of the full-length 14kb *DMD* transcript takes about 10 hours, the timing having been lowered from the estimated 16 hours due to recent data. Interestingly, the exonal region of the *DMD* gene is less than 1% of the complete gene; the rest consists of long intronic sequences [3,4]. In DMD, frameshift mutations lead to lack of dystrophin production, 60% of those mutations occurring between exons 45 and 55 [5]. However, not all mutations lead to DMD; occasionally even larger deletions than those seen in DMD are seen in patients with a less severe form of muscular dystrophy, Becker muscular dystrophy (BMD). The reading frame hypothesis, proposed by Anthony Monaco, clarifies this; an out-of-frame deletion, which shifts the mRNA translation, leads to little or no protein production. Yet if the mutation is in-frame, then an internally truncated but functional protein will still be produced, despite the size of the deletion.

The 427-kDa dystrophin protein carries an NH2-terminal actin-binding domain proceeding spectrin-like repeats - a sequence of repeating alpha-helices folded into small rods [2]. The actual

protein is split into four main functional domains: the NH2 terminal, a central rod domain, a cysteine-rich domain, and a COOH-terminal domain [2,6]. The two calponin homology domains located at the NH2 terminal allow dystrophin to bind to F-actin. The central rod domain consists of 24 spectrin repeats, along with four proline-rich hinge regions. These hinge regions provide the protein with flexibility; H1 is located after the NH2 terminal, H2 between spectrin repeats 3 and 4, H3 between repeats 19 and 20, and H4 at the end of the central rod domain. Beta-dystroglycan, found at the sarcolemma, binds to dystrophin at the WW domain (located on H4) and two EF-hands (located in the cysteine-rich domain). The cysteine-rich domain binds to other molecules as well, including calmodulin and ankyrin-B [6]. Finally, the Carboxyl terminal domain contains alpha helical coiled coils that allow it to bind to dystrobrevin and syntrophins, members of the Dystrophin Glycoprotein Complex (DGC). In other words, dystrophin is an integral part of the DGC, anchoring the intracellular cytoskeleton to the extracellular matrix [7]. Components of the DGC consist of various proteins/glycoproteins, including dystroglycans, sarcoglycans, dystrobrevins, syntrophins, and sarcospan.

Briefly, there are two subunits of dystroglycan associated with the DGC: the extracellular alpha-dystroglycan and transmembrane beta-dystroglycan. Dystroglycan binds various proteins and is a major laminin receptor in muscle. As mentioned above, it is the beta-dystroglycan subunit that binds dystrophin. Atypical dystroglycan glycosylation is associated with numerous disorders, including various muscular dystrophies [8]. There are four transmembrane sarcoglycan subunits - alpha, beta, gamma, and delta. Among other functions, sarcoglycan associates with beta-dystroglycan and forms a complex with sarcospan. Alpha-dystrobrevin is expressed in muscle and the brain; beta-dystrobrevin, encoded by a different gene, is expressed in other tissues. This component of the DGC interacts with dystrophin, and lack of dystrobrevin is

implicated in various disorders, including myotonic dystrophy type 1 (DM1) [8]. Syntrophins recruit various signaling proteins. At the DGC, syntrophins associate with the rod domain and anchor nNos, as well as bind to the C-terminal of dystrophin [9]. Finally, Sarcospan – a member of the DGC that was complicated to identify initially - is a transmembrane protein that interacts with sarcoglycans to assemble the DGC; they form a subcomplex [10]. Additionally, sarcospan influences alpha-dystroglycan glycosalation and laminin binding at the sarcolemma. Furthermore, sarcospan can stabilize the sarcolemma in dystrophic-deficient *mdx* mice, whereas lack of sarcospan can exacerbate the disease [11, 12]. Because the DGC anchors the intracellular cytoskeleton to the extracellular matrix, the absence of even one major component will compromise the integrity of the membrane.

DMD presents in boys during childhood, around 4 years of age, with a progressive proximal muscle weakness leading to loss of ambulation by age 12, along with calf hypertrophy and an increase in serum creatine kinase [13]. As the disease progresses death ensues due to respiratory insufficiency or cardiomyopathy, usually in the second or third decade [1,14].

A less severe form of muscular dystrophy, BMD, is also an X-linked recessive disorder caused by a mutation in the *DMD* gene [14, 15]. BMD mutations are in-frame, which leads to the production of an internally truncated but functioning protein. BMD is progressive, yet the progression is slower. Muscle degeneration and necrosis, followed by adipose tissue replacement and fibrosis, occur in BMD as well. In BMD, ambulation is not lost by age 12 and the amount of muscle weakness is variable [14]. Additionally, the length of survival is longer in BMD than DMD. Because of this, various methods have been devised to turn a DMD phenotype into a BMD phenotype. One such method is CRISPR/Cas9, which is the basis for this project.

Introduction

Duchenne muscular dystrophy (DMD) and Becker muscular dystrophy (BMD) are two examples of more than 30 types of muscular dystrophies [16]. In addition to symptoms, DMD and BMD have similar pathology, but BMD is milder than DMD. In both cases, the muscle cells die and are replaced by fat and fibrosis; myonecrosis and regeneration occur in relation to inflammation and repair. More specifically, lack of dystrophin leads to a compromised sarcolemma that can no longer accommodate mechanical stresses of muscle contraction. Intracellular calcium levels can then increase, activating necrosis. Following necrosis, these fibers can be targets of M1 macrophages [17]. M1 macrophages can also signal other inflammatory cells to the site to further exacerbate the inflammation. Compared to healthy subjects, TNF-alpha is increased 1000 times in DMD patients [18]. Additionally, Il-6 levels also rise, and is age dependent. IL-10, IL-17, IFN-gamma, Transforming Growth Factors (TGF), and chemokines are upregulated in DMD, as well [18].

Standard of care for DMD includes the anti-inflammatory corticosteroids prednisone or deflazacort [19]. Corticosteroids are lipophilic and can easily diffuse across the cell membrane [20]. These steroids can improve strength and pulmonary function, prolong ambulation, delay cardiomyopathy and improve motor function [19, 21]. Despite the benefits of glucocorticoid treatment, however, chronic treatment can produce severe side effects. Moreover, pharmacological intervention does not stop the disease progression, and chronic administration can lead to weight gain, compromised height, bone mineral density reduction (an effect seldom observed in patients who are not on steroids), osteoporosis, cataracts, and changes in behavior [22].

One treatment for DMD is an approach called anti-sense oligo mediated exon skipping. This approach attempts to restore dystrophin expression by taking the out-of-frame *DMD* mRNA and, using the anti-sense oligo, tricking the cellular machinery to alter splicing and restore the reading frame. To do this, oligonucleotides are generated to mask a specific exon, so that it is not included in the mRNA splicing [23]. This treatment is FDA approved, yet it is not a permanent solution since it does not manipulate the mutated DNA and only works on the RNA level.

Another method - to compensate for the lack of dystrophin in DMD - is administration of micro-dystrophin via an adeno associated viral vector (AAV). Due to AAVs limited packaging capacity, the full-length dystrophin is too large and approximately 70% of the cDNA must be deleted to fit into AAV. Therefore, functional microgenes were reported in the early 2000s by the Xiao lab and Chamberlain lab [24]. Further improvements on the gene have been made to increase its therapeutic benefits. However, though dystrophin expression is restored with micro-dystrophin administration, like exon skipping, this mode of therapy is not a permanent solution since it does not modify the patient's inherent DNA. A permanent solution is CRISPR/Cas9-mediated therapy.

Clustered regularly interspaced palindromic repeats (CRISPRs) were detected in various organisms, such as bacteria and archaea. The CRISPR/Cas system is used as an adaptive immune system against foreign DNA [25]. In this mechanism, the invasive DNA is captured and added as a new spacer in the prokaryotic DNA. This new spacer is then transcribed into CRISPR RNAs that associate with a Cas nuclease. Together, this complex can recognize and terminate the foreign DNA [26]. Researchers have adapted this system to enable targeting and double-stranded cutting of mammalian DNA, allowing gene editing of specific loci on the DNA [25].

Guide RNAs can be used to delete one or more exons, by targeting them to flanking introns. The cut sites are repaired by non-homologous end joining to restore the reading frame. In this scenario, a Cas9 will cut at the two flanking introns and remove the out-of-frame mutation before the two ends of the remaining DNA bind to each other, leading to an internally truncated but functional dystrophin protein, such as that seen in BMD.

Many studies have used CRISPR/Cas9 to demonstrate the potential therapeutic benefit for DMD. Li et al., Ousterout et al., and Young et al. are just some examples of notable groups who worked with CRISPR/Cas9 on the *DMD* gene to skip either exon 45 or 45-55, respectfully. Other deletions of various exons have also been accomplished [27, 28].

Since about 60% of the mutations in DMD occur between exons 45 and 55, removing this region to restore the reading frame can help the majority of patients. Young et al. show successful deletion of this region in human induced pluripotent stem cell (hiPSC) lines, and how skeletal muscle and cardiac muscle derived from hiPSC express a functional dystrophin [28]. To conduct this study, Young et al. designed various gRNAs to target *DMD* introns 44 and 55, including, notably, 44C4 and 55C3. They did so to target as many base pairs as they could, leaving only around 500 bp of each intron flanking either exon 44 or 56.

Although the CRISPR/Cas9 system is a powerful tool to manipulate DNA, there is a chance for imprecise targeting since the nuclease may cut a site even if there is imperfect complementarity with the guide RNA [29]. For this reason, variants of Cas9 have been generated to improve the specificity of the system. Slaymaker et al. describe a variant called eSpCas9. The group rationalized that since the wild type *Streptococcus pyogenes* Cas9 (SpCas9) structure contains a positively charged groove between several of its domains (HNH, RuvC, and PAM-interacting domains), it has a greater chance of interacting with the negativity of, and acting on, the non-

target regions. They hypothesized that by neutralizing this region, the gRNA-non target association would decrease, and the specificity for the target region would strengthen. They generated and identified a few mutants that had high efficiency (the on-target interaction was similar to wild type) and specificity (no off-target effects). One of these was "enhanced specificity" SpCas9, eSpCas9(1.1) [SpCas9 (K848A/K1003A/R1060A)]. To summarize, Slaymaker et al. showed that by neutralizing the groove, there were indeed less off-target effects while the efficiency of cutting did not decrease.

Another variant is Hyper-accurate Cas9 (HypaCas9), described by Chen et al. [30]. The theory behind the generation of HypaCas9 is as follows: when bound to on-target sites, the HNH region of the SpCas9 undergoes a conformational change, whereby it is trapped in an inactive state when bound to a mismatched target; however, the HNH region isn't in contact with the nucleic acids that sense base-pair complementarity. Rather, it is REC3 that recognizes the RNA/DNA heteroduplex and influences the HNH activation. Additionally, when the Cas9 is bound to an off-target region, the REC2 domain keeps the HNH domain in the checkpoint conformation. By exploiting this mechanism, Chen et al. showed that HypaCas9, which consists of a cluster of residues in REC3 with an alanine substitution for each residue (N692A, M694A, Q694A, H698A), has greater specificity compared to WT SpCas9 and equivalent or better specificity compared to other Cas9 variants, including eSpCas9(1.1).

The purpose of this study is to evaluate whether high fidelity nucleases like eSpCas9 and HypaCas9 are as efficient as wild type SpCas9. Here I test and compare the efficacy of wild type SpCas9, eSpCas9(1.1), and HypaCas9 on introns 44-55 of the *DMD* gene. Since both HypaCas9 and eSpCas9(1.1) maintain efficiency equivalent to wild type SpCas9 when tested in other

systems [29,30], I hypothesize that the *DMD* intron 44-55 editing will remain equivalent to that of SpCas9.

Materials and Methods

Cloning

The first step in this study was to generate plasmids containing the sequences encoding for gRNA and Cas9. Due to Young et al.'s work, the Spencer Lab already had a plasmid encoding for 44C4 (the guide targeting intron 44) and wild type SpCas9 as well as a plasmid encoding for 55C3 (the guide targeting intron 55) and SpCas9. The following describes the methods taken to clone the gRNA into a plasmid with either eSpCas9(1.1) or HypaCas9.

44C4 or 55C3 into eSpCas9(1.1)

Sense and antisense oligonucleotides for the gRNA 55C3 were annealed using 2.5µl of each, 1.0µl of 10X annealing buffer, and 4.0µl ddH2O. The solution was incubated at 95°C for 4 minutes and then at room temperature for 15 minutes. Following the annealing process, 0.8µl of BbsI was used in conjunction with 2.5µl T4 ligase buffer, 1.0µl NEBuffer 2.1, 0.8µl of the annealed oligonucleotide, and 500ng of the DNA encoding for eSpCas9(1.1). The sequence from 245bp until 267bp on the backbone containing eSpCas9(1.1) was digested out. The annealed oligonucleotide encoding for 55C3 was ligated in its place. Stbl3 cells were transformed with 2.5µl of the plasmid. The bacteria were inoculated and incubated and shook (at 190 RPM) in 37°C overnight. The following day, a miniprep was conducted to extract the DNA from the bacteria.

The above methods were repeated with 44C4 (using different primers designed for 44C4) to clone the sequence encoding for this gRNA into the eSpCas9(1.1) backbone.

44C4 into HypaCas9

A polymerase chain reaction (PCR) was conducted to amplify the HypaCas9 region of the BPK4410 – human expression plasmid for SpCas9 Cluster 1 (HypaCas9) and another PCR was conducted to amplify the region containing 44C4 of the plasmid with wild type SpCas9. To amplify the HypaCas9 region, 2.5µl of 10X AccuPrime PCR Buffer I, 0.7µl forward primer for HypaCas9, 0.7µl reverse primer for HypaCas9, 5.0ng DNA, 0.5µl Accuprime TAQ Polymerase,1.0µl DMSO, and 17.6µl ddH2O was used. The steps and volumes as above were repeated using a primer and reverse primer for the region on the backbone containing 44C4 and the appropriate DNA.

The PCR was run on a Bio-Rad T100 thermal cycler as follows: 1) the initial denaturation step of the PCR was run at 94°C for 1:30 min. 2) Denaturation was conducted at 94°C for 0:30 minutes. 3) The annealing temperature was 60° for 0:30 minutes with an extension time of 2 minutes per kb (10 minutes in total) at 68°C; the denaturation, annealing, and extension steps were run for 34 cycles followed by a 4°C infinite hold until the product was used for cloning.

An NEBuilder Hifi DNA Assembly Master Mix was used to assemble the 44C4 and HypaCas9 backbone. Once the complete plasmid was generated, 5-alpha competent cells were transformed with 2.5µl of the plasmid and plated, followed by inoculation and overnight shaking and incubation at 37°C. A miniprep with Sigma GenElute was conducted thereafter, followed by sequencing.

55C3 into HypaCas9

The backbone containing the sequence for 55C3 and SpCas9 was used, as was the product from the earlier step containing the sequence encoding for 44C4 and HypaCas9. The gRNA of both plasmids were digested out of their respective plasmids using, per sample, 12.0µl ddH2O, 5.0µl DNA, 2.0µl NEBuffer 3.1, 0.5µl NotI, and 0.5µl XBAI. The samples were incubated at 37°C for 1 hour.

Following the digestion, the products were run on a 1% agarose gel. The 55C3 fragment and the HypaCas9 fragment were extracted in the same tube using an Invitrogen Purelink Quick Gel Extraction Kit. The two extracted fragments were then ligated together using 5.0µl of the extracted DNA (which contains both fragments), 4.0µl 5X T4 DNA Ligase Buffer, 1.0µl T4 DNA Ligase, and 10.0µl ddH2O. The sample was incubated at 14°C overnight. The following day, Stbl3 cells were transformed with 2.5µl of the ligated product and plated. Following inoculation and 37°C incubation overnight, a miniprep with Sigma was conducted and the eluted DNA was sent for sequencing.

Maxiprep

Once all four plasmids described above were generated, a maxiprep using Qiagen, eluting with 400µl of water, was conducted for each plasmid. 10.0µl of each product was then run on a 1% agarose gel to confirm DNA presence.

In Vitro Cell Culture

Six plasmids were used to test the efficacy of cutting on the *DMD* gene in vitro. 55C3 + SpCas9, 44C4 + SpCas9, 55C3 + eSpCas9(1.1), 44C4 + eSpCas9(1.1), 55C3 + HypaCas9, and 44C4 + HypaCas9. The DNA concentrations of each were determined via spectrophotometry.

Transfecting HEK293 Cells

The HEK293 cell medium contains 87% DMEM, 10% FBS, 1% 100X Glutamax, 1% P/S, and 1% Nonessential Amino Acid. The media is stored at 4°C.

1.0ml of thawed HEK293 cells was transferred into a 15ml conical tube with 3.0ml medium prior to seeding in a flask containing 7.0ml medium. The cells were transfected in triplicates at around 60% confluency, with 2.0ng/well, using two12-well plates, three wells for each plasmid (except for 44C4 +SpCas9,which had 6 wells but only 3 were used in TIDE analysis), including 55C3 + SpCas9, 44C4 + Spcas9, 55C3 + eSpCas9(1.1), 44C4 + eSpCas9(1.1), 55C3 + HypaCas9, and 44C4 + HypaCas9. Three wells were used as a GFP control. 200µl of Opti-MEM media along with 6.0µl of Viafect transfection reagent per well was used to facilitate the transfection.

The cells were split into new wells at 24 hours post transfection and were harvested 48 hours post transfection. The DNA from the harvested HEK293 cells was isolated using a Zymo Quick DNA Miniprep protocol.

PCR

PCR was conducted to amplify the intron 44 or intron 55 regions of the isolated DNA, depending on which gRNA was included in the transfection. Forward and reverse primers were generated to target these regions. The following volumes are for each sample: 2.5µl 10X AccuPrime Buffer II, 0.5µl forward primer, 0.5µl reverse primer, 0.16µl AccuPrime TAQ DNA Polymerase High Fidelity, 2.0µl DNA, 19.34µl water, for a total of 25µl.

The PCR was run on a Bio-Rad T100 thermal cycler as follows: 1) The initial denaturation was run at 95°C for 3:00 minutes. 2) Denaturation was run at 95°C for 0:30 minutes. 3) Annealing was run at 55°C for 0:30 minutes. 4) Extension was run at 72°C for 1:20 minutes. Steps 2-4 were repeated 36 times. A final extension was run at 72°C for 5:00 minutes followed by a 4°C infinite hold for several minutes until 4.0µl of each sample was used to run a 1% agarose gel to confirm successful amplification (figure 3).

The DNA was extracted from the gel using a Thermo Scientific GeneJET Gel Extraction Kit. The DNA was then sent for sequencing and TIDE analysis (TIDE analysis was conducted using the website http://shinyapps.datacurators.nl/tide/).

Statistics

The statistics used was a one-way ANOVA with a Tukey post-hoc (multiple comparison test). Significance is considered if $P<0.05$.

Results

To test and compare the efficacy of the Cas9 variants (wild type SpCas9, eSpCas9(1.1), and HypaCas9), plasmids containing the sequence encoding for a specific gRNA as well as a single Cas9 variant were generated. The gRNA 44C4 and 55C3 were successfully cloned into the eSpCas9(1.1) vector (figure 1). Using PCR, 44C4 was cloned into the BPK4410 – human expression plasmid for SpCas9 Cluster 1 (HypaCas9). Similarly, via co-digestion and ligation, 55C3 was cloned into a different BPK4410 – human expression plasmid for SpCas9 Cluster 1 (HypaCas9). The Spencer Lab already had plasmids containing the sequence for either 44C4 or 55C3 and wild type SpCas9, so there was no need to generate them again.

In total we had 6 plasmids, each with a distinct sequence encoding for either; 55C3 + SpCas9, 44C4 + Spcas9, 55C3 + eSpCas9(1.1), 44C4 + eSpCas9(1.1), 55C3 + HypaCas9, or 44C4 + HypaCas9. These plasmids were transfected into HEK293 cells, with a GFP control to test the efficacy of transfection (figure 2). The cells were harvested 48 hours post transfection, the DNA isolated, amplified (figure 3), and sent for sequencing. Following sequencing, the efficacy of the variants was tested using TIDE analysis.

There was no difference in editing efficiency between the eSpCas9(1.1) and SpCas9 when assessing gRNA 44C4 whereas there was a significant decrease in efficiency for HypaCas9 compared to eSpCas9(1.1) (figure 4A).

For 55C3 there was also no difference in the editing efficiency between eSpCas9(1.1) and SpCas9. However, there was a decreased editing efficiency for HypaCas9 compared to both eSpCas9(1.1) and wild type SpCas9 (figure 4B).

To test the eSpCas9(1.1) in vivo, I had to first clone the fragment encoding for this Cas9 into a pAAV-CK8 backbone. The Spencer Lab had this vector which also included the sequence encoding for wild type SpCas9. I opted to use TOPO cloning to clone the eSpCas9(1.1) sequence into a pCR 2.1-TOPO vector before digesting out the eSpCas9(1.1) fragment and attempting to ligate it into the pAAV-CK8 backbone. I used a TOPO TA Cloning Kit from Invitrogen. Following this protocol, I sent the product for sequencing to confirm the presence of eSpCas9(1.1). Surprisingly, the Cas9 was not eSpCas9(1.1). Instead, it was identical to wild type SpCas9. After further investigation, it was determined that the company that had sent us the eSpCas9(1.1) had mistakenly sent us the wrong plasmid. Being that I was new to the lab when I started working with it, it had not occurred to me to sequence the eSpCas9(1.1) before beginning my experiments. On the other hand, HypaCas9 was sequenced and its presence confirmed during the initial cloning phase. Therefore, though the findings for eSpCas9(1.1) described here are not viable, the results for HypaCas9 against wild type SpCas9 are.

Discussion

Young et al. developed gRNAs targeting *DMD* introns 44 and 55, to delete exons 45 through 55 of the *DMD* gene [28]. This single deletion can benefit the majority of DMD patients, since 60% of mutations in the *DMD* gene occur in this region. Young et al. tested their CRISPR/Cas9 platform using wild type SpCas9. To compare the efficacy of SpCas9 to two Cas9 variants (eSpCas9(1.1) and HypaCas9), I transfected HEK293 cells using 6 different plasmids, each containing a specific gRNA (either 44C4 or 55C3) as well as a Cas9.

In the published work, both eSpCas9(1.1) and HypaCas9 showed equivalent efficacy to wild type SpCas9 [29, 30]. However, though those studies were conducted on human cells, they were done on alternate genes, not the *DMD* gene. In the present study, when paired with 44C4, neither eSpCas9(1.1) nor HypaCas9 showed a significant difference in editing efficiency compared to wild type SpCas9, though there was a trend towards decreased efficiency for HypaCas9 and a trend towards increased efficiency for eSpCas9(1.1) When paired with 55C3, however, HypaCas9 showed a significant decrease in cutting efficiency compared to both, eSpCas9(1.1) and wild type SpCas9.

The gRNA binding of the DNA and the unwinding of the protospacer follow the binding of the Cas9 to the protospacer adjacent motif (PAM) sequence [31]. Since the unwinding occurs prior to the cleavage, the unwinding is important for Cas9 specificity. Okafor et al. performed an unwinding assay to determine why there is variation in genome editing with different Cas9/gRNA pairs. They determined that HypaCas9 has a decreased unwinding specificity compared to other Cas9 variants. This unwinding deficit could be implicated in the results of the

experiment described here, where HypaCas9 showed a decreased efficacy of cutting compared to wild type SpCas9 and eSpCas9(1.1).

Future Directions

The next step of this study is to test and compare the efficacy of the Cas9 variants in vivo. I started this process shortly after obtaining the results of the in vitro experiments. For this next step, I was to identify the Cas9 variant with equivalent or better editing efficacy compared to wild type SpCas9 in vitro and use this in vivo, again, against the wild type SpCas9. Based on the results, the obvious choice was eSpCas9(1.1). However, due to a mishap by the company who sent us the eSpCas9(1.1), the experiments for eSpCas9(1.1) described here will need to be repeated with the right plasmid. I hypothesize that there shouldn't be much of a difference to the results described above because eSpCas9(1.1) has been shown to have similar editing efficacy to wild type SpCas9.

Following the repeat of the in vitro studies, the correct eSpCas9(1.1) sequence should be cloned into a pAAV-CK8 backbone and used for in vivo experiments with a humanized dystrophic mouse model, as described in [32].

Nevertheless, on-target efficacy is only half the issue. Fidelity (off-target effects) is the other half. Following the above-described experiments, as long as eSpCas9(1.1) has the same or better efficacy compared to SpCas9, then whole-genome wide sequencing should be conducted following treatment with wild type SpCas9 or eSpCas9(1.1) to test for off-target effects. If eSpCas9(1.1) shows equivalent or better efficacy and less off-target effects than wild type

SpCas9, then eSpCas9(1.1) might be a better alternative than wild type SpCas9 for the treatment of the majority of DMD patients with a single exon 45-55 deletion.

Figures

A

B

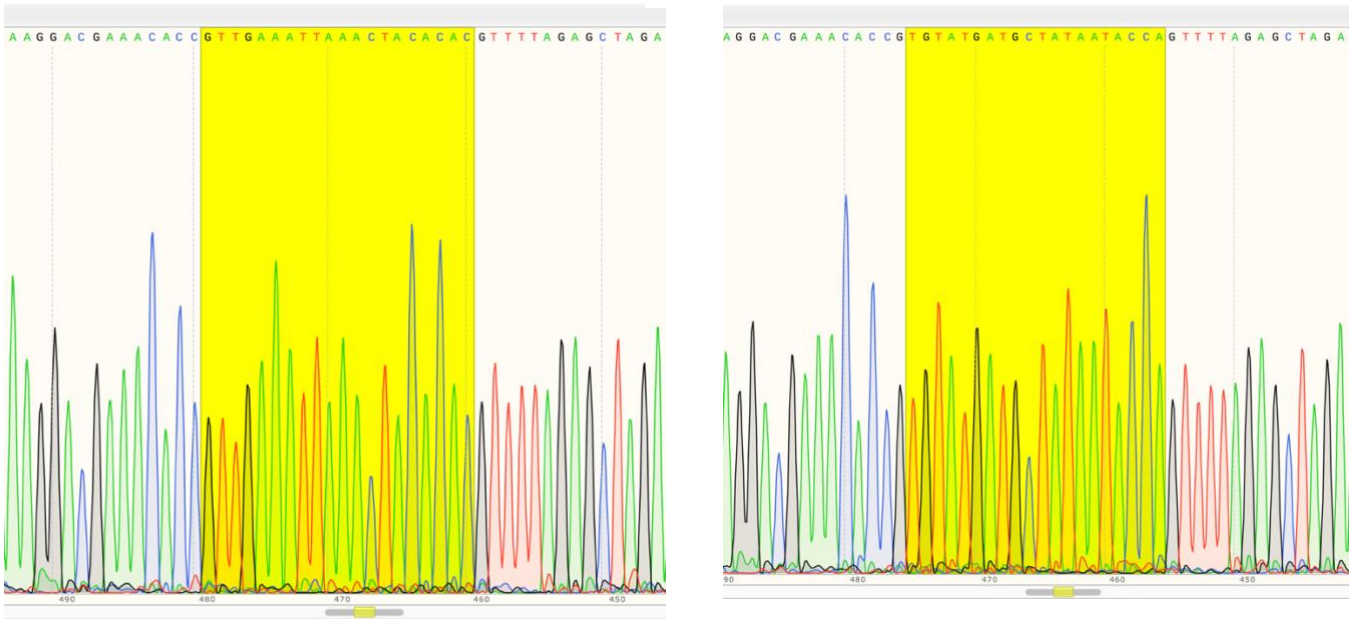

Figure 1: Successful cloning of gRNA into eSpCas9 backbone. The sequencing results of cloning A) 44C4 into the backbone containing eSpCas9(1.1) and B) 55C3 into the backbone containing eSpCas9(1.1). The yellow region is the sequence of the gRNA, the white are the flanking bp of the plasmid. Similar results were observed for HypaCas9 (not shown due to identical sequencing to figures 2A and 2B).

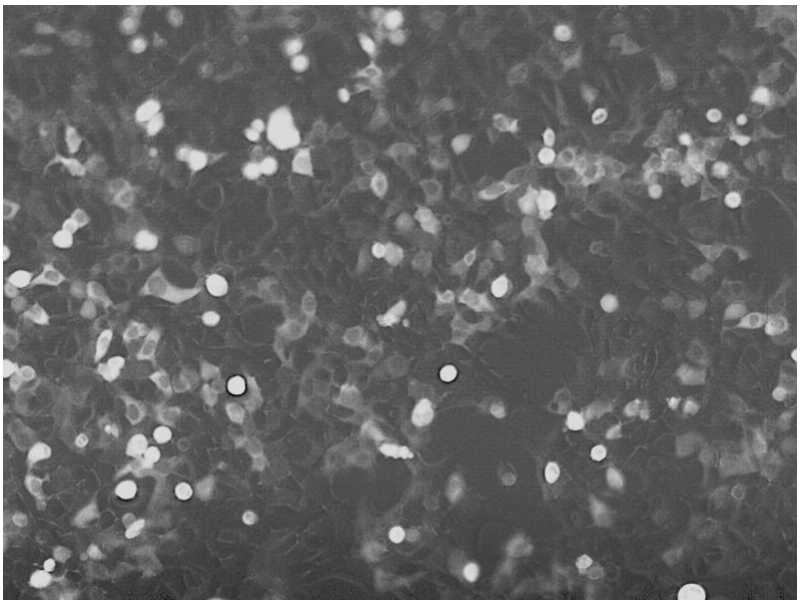

Figure 2: GFP control for efficacy of transfection. To test the efficacy of transfection of HEK293 cells, GFP was used as a control. Figure 2 shows the transfection efficiency 48 hours post transfection.

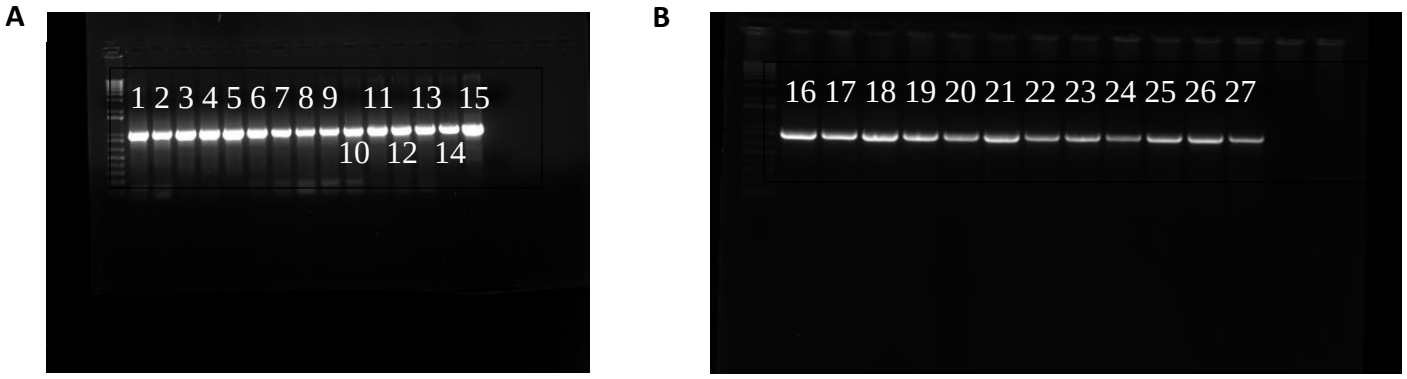

Figure 3: 1% agarose gel shows successful amplification of the 44C4 or 55C3 region post-harvest. Transfected HEK293 Cells were harvested 48 hours post transfection. The DNA was extracted using a Zymo Quick DNA Miniprep protocol, followed by PCR to amplify the intron 44 (figure 3A) or intron 55 (figure 3B) region. There are three wells per each plasmid (except 44C4+ SpCas9, which has 6 wells but only the DNA from wells 10, 11, and 12 were used for TIDE analysis, for consistency) and 3 wells for the GFP control, including 44C4 + SpCas9, 44C4 + eSpCas9, 44C4 + HypaCas9, and GFP control. 55C3 + SpCas9, 55C3 + eSpCas9, 55C3+HypaCas9, and GFP control. Using a 1kb ladder, the numbered wells include: wells 1-3= 44C4 + HypaCas9; wells 4-6 = 44C4 + eSpCas9; wells 7-12 = 44C4 + SpCas9; wells 13-15 = GFP control; wells 16-18 = 55C3 + eSpCas9; wells 19-21 = 55C3+HypaCas9; wells 22-24 = 55C3 + SpCas9; wells 25-27 = GFP control.

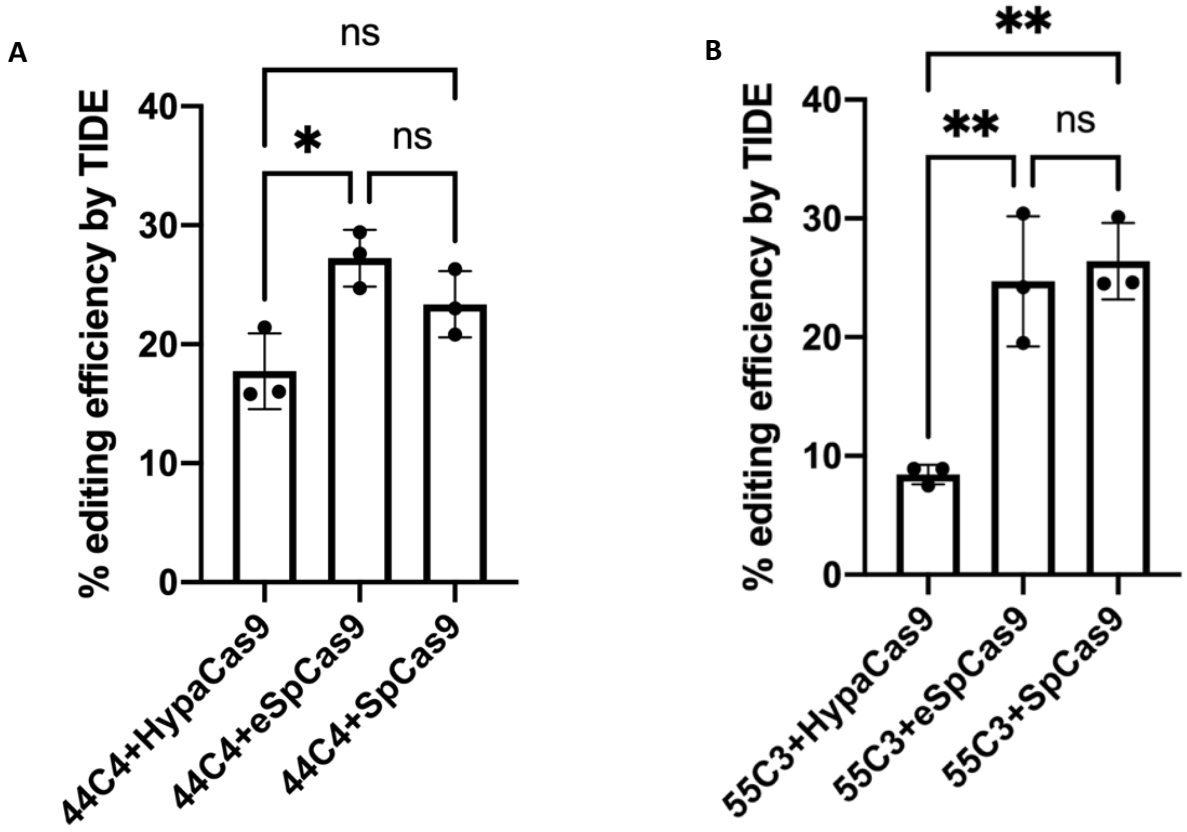

Figure 4: Editing efficiency of Cas9 variants paired with either 44C4 or 55C3. Using TIDE analysis, the editing efficiency of HypaCas9, eSpCas9, and SpCas9 were analyzed. Figure 4A shows the editing efficiency of the Cas9 variants paired with 44C4. Though there is a downward trend for HypaCas9 compared to wild type SpCas9, there is no significant decrement of editing efficiency. However, eSpCas9, despite being similar to SpCas9, does have a greater editing efficiency than HypaCas9. Figure 4B shows the editing efficiency of the Cas9 variants paired with 55C3. eSpCas9 has an equivalent editing efficiency to wild type. HypaCas9 shows a lower efficiency compared to both eSpCas9 and wild type SpCas9.

REFERENCES

1. Vijay Venugopal, Steven Pavlakis, *Duchenne Muscular Dystrophy*. In: StatPearls [Internet]. Published 19 November 2020.
2. Derek J. Blake et al. *Function and Genetics of Dystrophin and Dystrophin-Related Proteins in Muscle.* In: American physiological society. Published 01 April 2002
3. Sylvie Tuffery-Giraud et al. *Normal and altered pre-mRNA processing in the DMD gene.* In: Human Genetics (Springer). Published online 09 June 2017
4. Isabella Gazzoli et al. *Non-sequential and multi-step splicing of the dystrophin transcript.* In: RNA Biology. Published 21 February 2016
5. Andrew H. Ahn and Louis M. Kunkel, *The structural and functional diversity of dystrophin*. In: Nature Publishing Group. Published 01 April 1993
6. Quan Q Gao and Elizabeth M McNally, *The Dystrophin Complex: structure, function, and implications for therapy.* In: Comprehensive Physiology. Published online 24 June 2015
7. Hina F Bhat et al. *ABC of multifaceted dystrophin glycoprotein complex (DGC).* In: Journal of Cellular Physiology. Published 02 May 2017
8. Marta Gawor, Tomasz J. Prószyński. *The molecular cross talk of the dystrophin-glycoprotein complex.* In: ANNALS of THE NEW YORK ACADEMY OF SCIENCES. Published 25 October 2017
9. Marvin E Adams et al. *Syntrophin binds directly to multiple spectrin-like repeats in dystrophin and mediates binding of nNOS to repeats 16-17,* In: HUMAN MOLECULAR GENETICS. Published 22 May 2018

10. Hamie Marshall and Rachelle H Crosbie-Watson. *Sarcospan: a small protein with large potential for Duchenne muscular dystrophy.* In: Skeletal Muscle. Published online 03 January 2013
11. Angela K. Peter et al. *Sarcospan reduces dystrophic pathology: stabilization of the utrophin-glycoprotein complex.* In: Journal of Cell Biology. Published 03 Nov 2008
12. Elizabeth M Gibbs et al. *Loss of sarcospan exacerbates pathology in mdx mice, but does not affect utrophin amelioration of disease.* Published 11 January 2021
13. Eppie M Yiu et al. *Duchenne muscular dystrophy.* In: Journal of Paediatrics and Child Health. Published: 09 March 2015
14. Kevin M. Flanigan MD, *Duchenne and Becker Muscular Dystrophies*. In: ScienceDirect. Volume 32, Issue 3. Published August 2014
15. Giuseppe Lanza et al. *Motor activity and Becker's muscular dystrophy: lights and shadows.* In: The Physician and Sportsmedicine. Published online: 20 October 2019
16. Kristin Wilson et al. *Duchenne and Becker muscular dystrophies: a review of animal models, clinical endpoints, and biomarker quantification.* In: Toxicologic Pathology: SAGE journals. Published October 3, 2017
17. Oriana del Rocío Cruz-Guzmán et al. *Systemic Inflammation in Duchenne Muscular Dystrophy: Association with Muscle Function and Nutritional Status.* In: Hindawi, BioMed Research International. Published 24 Aug 2015
18. Boel De Paepe and Jan L. De Bleecker. *Cytokines and Chemokines as regulators of Skeletal Muscle Inflammation: Presenting the Case of Duchenne Muscular Dystrophy*. In: Hindawi, Mediators of Inflammation. Published 05 Nov 2013

19. Andrea M. Reinig et al. *Advances in the Treatment of Duchenne Muscular Dystrophy: New and Emerging Pharmacotherapies.* In: Journal of the American College of Clinical Pharmacy. Published 02 February 2017
20. M.A. Khan. *Corticosteroid therapy in Duchenne muscular dystrophy.* In: Journal of the Neurological Sciences. Published 1 December 1993.
21. Eric P. Hoffman, PhD et al. *Novel Approaches to Corticosteroid Treatment in Duchenne Mucular Dystrophy.* In: Physical Medicine and Rehabilitation Clinics of North America. Published November 2012
22. Corrado Angelini and Enrico Peterle. *Old and new therapeutic developments in steroid treatment in Duchenne muscular dystrophy.* In: Acta Myologica (Myopathies, Cariomyopathies, and Neuromyopathies). Published May 2012
23. Lucı́a Echevarrı́a et al. *Exon-skipping advances for Duchenne muscular dystrophy*. In: Human Molecular Genetics. Published 16 May 2018
24. Dongssheng Duan. *Systemic AAV Micro-dystrophin Gene Therapy for Duchenne Muscular Dystrophy.* In: Molecular Therapy. Published online on 17 July 2018
25. Jennifer A Doudna and Emmanuelle Charpentier. *Genome editing. The new frontier of genome engineering with CRISPR-CAS9.* In: Science. Published 28 November 2014
26. Philip M. Nussenzweig and Luciano A. Maraffini. *Molecular Mechanisms of CRISPR-Cas Immunity in Bacteria.* In: Annual Review of Genetics. Published 28 August 2020
27. Kenji Rowel Q. Lim. *Applications of CRISPR/Cas9 for the Treatment of Duchenne Muscular Dystrophy.* In: Journal of Personalized Medicine. Published 24 November 2018

28. Courtney S. Young et al. *A single CRISPR-Cas9 deletion strategy that targets the majority of DMD patients restores dystrophin function in hiPSC-derived muscle cells.* In: Cell Stem Cell. Published 07 April 2016

29. Ian M. slaymaker et al. *Rationally engineered Cas9 nucleases with improved specificity.* In: Science. Published 01 January 2016

30. Janice S. Chen et al. *Enhanced proofreading governs CRISPR-Cas9 targeting accuracy*. In: Nature. Published 19 Oct 2017

31. Ikenna C Okafor et al. *Single molecule analysis of effects of non-canonical guide RNAs and specificity-enhancing mutations on Cas0-induced DNA unwinding.* In: Nucleic Acids Research. Published 16 December 2019

32. Courtney S. Young et al. *Creation of a Novel Humanized Dystrophic Mouse Model of Duchenne Muscular Dystrophy and Application of a CRISPR/Cas9 Gene Editing Therapy.* In: Journal of Neuromuscular Diseases. Published 20 May 2017